J. Comp. App. Res. Mech. Eng. Vol. X. No. X, pp. X-X, XXXX *DOI: 10.22061/jcarme.XXXX.XXXX.XXXX*

SRTTU

Journal of Computational and Applied Research in Mechanical Engineering

jcarme.sru.ac.ir

JCARME

ISSN: 2228-7922

Research paper

Investigation of the effects of additives kaolinite nanopowders and different gases in vegetable oil dielectric on NDPM-EDM for MSGNP/Al-7075 composites

Haneen Lateef[a] and Saad Mahmood Ali[b,*]

[a]*Production Engineering and Metallurgy Department. University of Technology, Baghdad, 19006, Iraq*
[b]*Biomedical Engineering Department. University of Technology, Baghdad, 19006, Iraq*

Article info:

Article history:

Received:	00/00/0000
Revised:	00/00/0018
Accepted:	00/00/0000
Online:	00/00/0000

Keywords:

Argon and Freon gases,

Material removal rate,

Electrode wear ratio,

Surface roughness,

White layer thickness

***Corresponding author:**
saad.m.ali@uotechnology.edu.iq.

Abstract

This study aims to investigate the influence of input parameters in wet-EDM and near-dry powder mixing electrical discharge machining (ND-PMEDM) on the performance of newly fabricated aluminum with microscopic slide glass nanoparticles (Al-7075/MSGNP) nanocomposites produced via stir-casting. The current study included air, argon, a mixture of argon and nitrogen, and Freon gases, utilizing vegetable oil as the dielectric medium. Kaolinite Nano powders were used as an additive in ND-PMEDM studies. Minitab 18 software was employed to develop a mathematical model and predict the response of material removal rate, electrode wear ratio, surface roughness, and white layer thickness. The maximum material removal rates achieved in the ND-EDM and NDPM-EDM were 29.425 mm³/min and 15.468 mm³/min, respectively, when utilizing Freon gas. The result exceeds the maximum value achieved with vegetable oil alone by 209.37%. The minimum electrode wear ratio achieved with Freon gas was 0.003 when combined with vegetable oil, and 5% and 10% $Al_2SiO_2(OH)_4$. The minimum SR recorded was 4.567 µm, achieved with the Freon additive gas in the dielectric, utilizing 10A, T_{on} of 800 µs, and vegetable oil with 0% Cp. Additionally, SR of 4.797 µm was noted when applying 5% $Al_2SiO_2(OH)_4$. The SR values obtained are 19.88% and 14.13% lower than the minimum value achieved with sole vegetable oil. The SEM analysis indicated a significant reduction in the average thickness of the recast white layer when employing ND-EDM techniques in comparison to the conventional wet-EDM method. The findings can be utilized to improve the performance and durability of components.

1. Introduction

The application of powder-mixed electrical discharge machining (PMEDM), wire-cut electrical discharge machining (W-EDM), rotary EDM, micro EDM, ultrasonic-assisted EDM, and dry EDM machining, all of which improve performance, has been a notable advancement in EDM [1-3]. EDM is a method that utilizes short bursts of electrical discharges between a tool electrode and a workpiece, both submerged in a dielectric fluid, to remove material through a thermo-electrical process. The material removal mechanism in EDM is an intricate process that encompasses numerous metallurgical and physical processes [4, 5]. The machinability of EDM is primarily influenced by its electrical conductivity properties rather than its mechanical capabilities. Dielectric fluid consumption affects the effectiveness of EDM and has an impact on the environment [6]. The choice of dielectric fluid, whether it is air or another type of gas, has a notable influence on the performance parameters of the machining process [7-9].

The primary settings of EDM control the quantity of electric discharges and the intensity of each discharge. By altering them, the material removal rate (MRR), tool (electrode) wear rate (TWR), precision of resulting dimensions, and obtained surface roughness (SR) can all be controlled [10]. Advances in analysis tools, measurement, computer science, and the ongoing research into environmentally friendly methods and materials have enabled a better understanding of the MRR process, reduced processing times, broadened the range of applications, and improved the manufacturing process and surface quality. Thus, in several partial employments, EDM has lately emerged as a competitive alternative machining method [11].

Despite the benefits of EDM, the process has a significant environmental impact and a notable downside. EDM-producing contamination during the machining comes mostly from using the dielectric fluid. After EDM processing, the used dielectric waste cannot be recycled and is highly hazardous [12-14]. Hazardous vapors and toxic emissions are produced during processing because of the dielectric's chemical reactions at high temperatures [15-17]. Poorly and heavily biodegradable materials are mixed in the dielectric media, and the emission of electromagnetic radiation will hurt the environment [18, 19]. This is in addition to the scarcity of petroleum products, the high prices, the risk of fires, and the need to increase the productivity of the process [20, 21].

To bridge this environmental gap, the present work focused on modifying the properties of the dielectric medium to achieve an environmentally friendly medium while improving the performance of the EDM output. It also focused on conducting a practical investigation of dry EDM and semi-dry EDM (ND-EDM) processes as two environmentally friendly alternatives to wet and mixed EDM processes [22].

One of the most important requirements of modern industry is the production of lightweight, high-strength materials and composite materials, which are the ideal solution for achieving these. Aluminum and its alloys are ideal examples of metallic materials due to their lightweight and high corrosion resistance [23]. The exceptional properties of aluminum alloys, their high specific strength, high thermal properties, and low density, make them widely used as industrial materials [24]. The demand for metal matrix composites (MMCs) has increased in various industries such as transportation, automotive, electrical, structural, and aerospace due to recent advancements. These composites are used in applications like engine pistons, cylinder liners, and disc brakes. The development of these materials is driven by their numerous advantages, including a high strength-to-weight ratio, toughness, and wear resistance [25-28]. However, there are some drawbacks associated with these composites, such as their hardness, brittleness, and the challenges in producing composite wafers [29, 30]. The main advantages of using aluminum MMCs for enhanced tribological properties, better coefficient of thermal expansion, better damping capabilities, and higher strength and stiffness [24]. Furthermore, more research is required to enhance the production process and facilitate the extensive application of these materials in a

variety of composite-based products due to their high cost [31–34].

The main objective of this research is to identify the best levels of input parameters for the wet, near-dry, and PMEDM processes. The factors involved include the current (I_p), pulse duration (T_{on}), and various dielectric mediums, such as vegetable oil with or without gaseous mixes like air, argon, mixed (argon + nitrogen), and Freon. The objective of the study is to investigate the impact of these factors on the strengthening mechanisms and surface integrity of the MMCs manufactured by the stir-casting technique as workpieces. The vegetable oil dielectric will be used in the current project to reduce the emission of harmful substances and prevent environmental pollution.

2. Materials and methodology

2.1 The workpieces MMCs preparation

The workpieces examined in this investigation are MMCs consisting of an aluminum (Al7075) alloy *matrix* reinforced with microscopic slide glass nanoparticles (MSGNP). Composite materials provide numerous advantages, such as outstanding hardness, a high strength-to-weight ratio, and corrosion resistance [35 and 36]. The Hanwei Company, situated in China, imported and thoroughly examined the aluminum alloy ingot. The ingot plate that was bought has dimensions of 500 mm in width, 200 mm in height, and a thickness of 2 mm. The plate was segmented into brief strips and subsequently positioned in an appropriate crucible for the process of stir casting. An essential aspect of this process is to achieve effective wetting between the molten metal and the particle reinforcement to provide a more homogeneous distribution of the reinforcing particles [37]. The glass powder, derived from microscope slides, served as the primary reinforcement in the form of nano-particles. The glass powder has been sieved to a size of 35 nm.

The composite samples were produced using the stir-casting method. This casting procedure was isolated using argon gas pumped through a side tube. The matrix (Al-7075) was first heated to 700°C in an electric smelting furnace. After the alloy was melted, magnesium chips were added to the molten metal, where magnesium vaporizes at 450°C. Glass particles warmed in the stir-casting furnace were gradually placed in the specified weight ratios into the slurry at 720°C and stirred using a stainless-steel stirrer to avoid powder agglomeration and ensure homogeneous dispersion.

The composite workpieces were analyzed through X-ray diffraction (XRD) analysis and scanning electron microscopy (SEM). The XRD technique was used to analyze the workpiece materials, employing the backloading preparation method [33]. Tensile testing was performed using the ASTM-E8 standard, utilizing a WDW-200E universal tensile testing machine. A load of 20 kN was applied, and the strain rate was set at 0.5 mm/min. The Rockwell hardness test, by the ASTM E-18 standard, was used to prepare test specimens for hardness testing. Specimens possessing a sleek surface were subjected to a 10-second indentation using a weight of 100 kg.

The chemical composition of the fabrication workpiece materials Al7075/MSGNP consists of aluminum, magnesium, iron, and silica. Glass nanoparticles were used to enhance the silica content, enhancing hardness, tensile strength, corrosion resistance, and rupture resistance at elevated temperatures. An important chemical reaction takes place between the MSGNP and aluminum particles.

An analysis of the microstructure of the composites, which are made up of Al7075 alloy and 8wt % nano clear glass powder, revealed a strong metallurgical bond between the aluminum particles. The adsorption of glass onto the aluminum matrix and the presence of other components were analyzed using SEM images and EDX patterns. The EDX analysis showed an increase in the composition of Si in the composites compared to the base material. The peaks for Na, C, and O represent the alloying components of the Al7075 base matrix. The results of the EDX study confirmed the presence of SiO_2 and oxidation, leading to the selection of the 8% composition for further analysis. According to EDX, Al 7075/MSGNP has the following chemical composition, which is shown in Table 1.

The highest ultimate tensile strength was observed when 4% MSGNP was used. This is because glass particles have a strong affinity for the aluminum matrix, resulting in excellent wettability. The composite containing 8% MSGNP exhibited the highest level of hardness. The reason for this is the existence of very rigid ceramics (MSGNP) particles within the aluminum alloy matrix. These particles impose a greater restriction on localized matrix deformation during indentation [38], and they are evenly distributed throughout the matrix. Tensile strength and hardness significantly improved and reached maximum values when glass nanoparticles were added to the Al7075 matrix at a weight ratio of 8%. The microstructure examination of Al7075 revealed strong metallic bonding between the aluminum particles, as well as the even distribution and transparency of glass particles at the ideal addition level. Consequently, a choice was made to utilize it as the substance for the workpiece during the subsequent investigation of the current project.

2.2 The wet, near dry, and PMND-EDM machining processes

This work investigates the utilization of practical experiments to determine the optimal machining parameters and the appropriate machining process, such as wet, near dry, and PMND-EDM approaches. The output performance measures consist of the MRR, electrode wear ratio (EWR), SR, and white layer thickness (WLT). The EDM studies were carried out using a die-sinking EDM machine, specifically the CHMER type CM 323C.

The hybrid configuration for wet, near dry, and PMND-EDM tests was internally designed by locally fabricating and preparing the required accessories. A significant achievement of this investigation was the creation of an additional attachment.

The attachment introduced a dielectric medium consisting of both liquid and gas phases between the tool and the workpiece. The system unit comprises various components, such as a gas cylinder, an air compressor, a gas filter, a milling vice for workpiece positioning, a tank for dielectric fluid storage, a pump for dielectric fluid recycling, multiple flexible tubes for high-pressure dielectric medium passage, a tool holder and filters for dielectric fluid purification. The air compressor supplied compressed air, while the gas cylinder released gas. The tank was filled with a suitable quantity of dielectric medium, specifically vegetable oil. The setup unit is equipped with gas and air pressure gauges that measure the operational pressure of the dielectric gas, ranging from 0.1 MPa to 0.5 MPa. The experiments were conducted using a dielectric medium, consisting of compressed air and dielectric oil. Plastic tubing was used to link the cylinder outlet to the hollow tool electrode. The gas was able to pass through the inter-electrode gap (IEG) and act as the necessary dielectric medium. Fig. 1 illustrates the diagram of the wet, ND-EDM, and NDPM-EDM processes and the newly constructed experimental facility. Table 2 contains the list of experimental parameters for each test.

Table 3 presents the physical characteristics of different dielectric materials, such as vegetable oil, air, argon, a blend of argon and nitrogen, and Feron. Nanoparticles of kaolinite ($Al_2Si_2O_5(OH)_4$) were introduced into the dielectric fluid for PMND-EDM testing. The utilization of the field emission scanning electron microscope (FE-SEM) allowed for the examination of powder blending and the evaluation of particle sizes. Fig. 2 exhibits the SEM image of the $Al_2Si_2O_5(OH)_4$ powders.

Table 4 presents the chemical makeup of $Al_2Si_2O_5(OH)_4$, while Table 5 offers details on the thermophysical properties and particle size of blended powder materials. For these experiments, a copper electrode equipped with an internal cleaning system was used.

Table 1. The chemical composition of Al7075/MSGNP by EDX.

Element	Wt.% composition	Element	Wt.% composition
Mg	1.12	Ni	0.01
Fe	0.22	Ti	0.02
Si	1.83	Na	2.1
Cu	1.37	C	0.02
Mn	0.14	O	0.01
Zn	5.84	Al	Balance

Fig. 1. The developed experimental facility for the wet, near-dry, and NDPM-EDM processes.

Table 2. The used NDPM-EDM, wet and near-dry processes parameters.

Process	Unit	Wet-EDM	NDPM-EDM
Dielectric medium	-	Vegetable oil	Vegetable oil + air, Ar, Ar + N, Fr]
Machining time	Sec	0.2	0.2
Discharge	A	10, 30	10, 30
Pulse on	µs	800, 1600	800, 1600
Pulse off	µs	800	800
Gap voltage	V	10	10
High voltage	V	140	140
Low voltage	A	30	30
Working	MPa	0.1-0.5	0.1-0.5
Jumping time	m/min.	0.4	0.4
Powder concentration	g/l	-	0%, 5%, 10%
Powder type	-	-	Kaolinite

• Workpiece electrode – Al metal matrix composite, tool electrode – copper

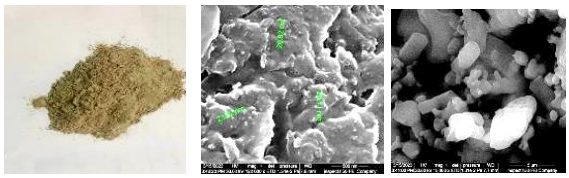

(a) (b) (c)

Fig. 2. The used $Al_2Si_2O_5(OH)_4$ powder additives (FE-SEM) tests (a) microscopic slide glass nanoparticles (MSGNP), (b) boron carbide (B4C), and (c) tungsten carbide (WC).

Table 3. The physical properties of dielectric fluids.

Dielectric	Density (kg/m^3)	Viscosity	Dielectric	Density (kg/m^3)
Air	1.229	$1.647\times10^{-}$	0.026	1006
Argon	1.622	$2.125\times10^{-}$	0.015	520.64
Nitrogen	1.138	$1.663\times10^{-}$	0.024	1040.67
Ferron	3.220	$2.791\times10^{-}$	0.109	840.20
Vegetable	919.21	$4.021\times10^{-}$	0.16	2171

Table 4. The chemical composition of $Al_2Si_2O_5(OH)_4$.

Element	SiO_2	Al_2O_3	Fe_2O_3	TiO_2
%	47.14	34.74	1.26	1.2
Argon	1.622	2.125×10^{-5}	0.015	520.64
Element	CaO	Mg	SO_3	Moisture
%	1.08	0.25	0.08	14.44

Table 5. Thermo-physical properties of the used $Al_2Si_2O_5(OH)_4$ powders.

Properties	Amount
Particle size (nm)	36.2
Color	Grey
Thermal conductivity (W/cm.°C)	0.222
Density (g/cm^3)	2.650
Boiling point (°C)	NA
Melting point (°C)	1760

The electrode was constructed from copper with a purity of 99%. It had a length of 55 mm with outer and inner diameters of 12 mm and 6 mm, respectively. The selection of copper as the material for the instrument was based on its exceptional electrical and thermal conductivity, as well as its simplicity of manufacturing and affordability. A sample was examined before cutting the copper electrode, and the findings are included in Tables 6 and 7.

3. Results and discussion

The data obtained from the EDM experimental work was utilized to create a mathematical model using Minitab 18 software. This model was then used to predict different response properties. The predicted results were analyzed and compared with the experimental values. Additionally, Analyses of Variance (ANOVA) were employed to determine the input parameters that had the most influence on each response.

Table 6. The chemical composition of copper electrode.

Zn%	Pb%	Sn%	Co%	P%	Fe%
0.0001	0.0005	0.0005	0.0004	0.0001	0.0091
Al%	S%	As%	Ag%	Mn%	Bi%
0.0024	0.0001	0.0001	0.0024	0.0002	0.0001
Ni%	Si%	Cr%	Cd%	Sb%	Cu%
0.0004	0.0373	0.0008	0.0001	0.0017	Residel

Table 7. The physical properties of copper electrode.

Physical properties	Values
Electrical conductivity (S/m)	58.5
Thermal conductivity at 20 °C (W/m.°C)	18
Electrical resistivity at 20 °C (Ωmm²/m)	0.017
Modulus of elasticity (GPa)	115
Thermal expansion coefficient (ppm/°C)	17.7
Melting point (°C)	1083
Density (g/cm³)	8.94

3.1. The experimental results for MRR, EWR, and SR using vegetable oil (Wet-EDM)

The experimental results from Table 8 were used to analyze the impact of input parameters (I_P) and (T_{on}) on the responses MRR, EWR, SR, and WLT when vegetable oil was used as a dielectric. The full factorial design (FFD) method and MINITAB 18 software were used to conduct these analyses. For all response parameters from the current research results, the lowest SR, lowest tool wear ratio (TWR), lowest white layer thickness (WLT), and highest material removal rate (MRR) are considered the best. The relationship between the current (I_p) and pulse-on-times (T_{on}) and the MRR are illustrated in Fig. 3(a to f), The metal removal rate values increase with increasing both the pulse current and the duration of the pulse. The MRR demonstrates an increase as the Ip is raised from 10 A to 30 A while keeping the pulse-on-times (T_{on}) constant at values of 800 µs and 1600 µs specifically, the MRR increases by 635.17% and 578.08% for the respective pulse-on-times mentioned, as depicted in Fig. 3(a to f). An incremental rise in the MRR values was noted as the T_{on} increased from 800 µs to 1600 µs, with a commensurate increase of 14.80% and 5.21% when utilizing pulse currents of 10A and 30A, as depicted in Fig. 3(b).

This phenomenon can be related to the fact that when the current values grow, more electrons collide with the workpiece, resulting in an elevation of the surface temperature. Consequently, a larger amount of material from the workpiece is eroded.

Higher current density increases pressure and temperature within the plasma channels, resulting in more erosion of the work material. The reason for this is the higher discharge energy of plasma channels and longer pulse durations, which leads to increased energy transfer to the electrodes. Consequently, the duration of the melting and evaporation process is extended, leading to an increased MRR for the selected fluids. The maximum MRR value attained was 35.612 mm³/min, which was seen at the highest levels of I_P (30 A) and T_{on} (1600 µs).

Fig. 3(c and d) demonstrates the correlation between the current (I_P) and pulse-on-time (T_{on}) and the EWR. The EWR value peaked at 2.573 mm³/min, coinciding with the highest values of I_P (30 A) and T_{on} (1600 µs). It has been shown that increasing the current (I_P) from 10 A to 30 A, with pulse-on-times of 800 and 1600 µs, results in a significant increase of 982.26% in the EWR, as depicted in Fig. 3(c).

The EWR increased by 603.76% and 27.82% when the utilized T_{on} was doubled from 800 µs to 1600 µs while keeping the pulse current constant at 10 A and 30 A, respectively, as shown in Fig. 3(d).

This phenomenon can be explained by the collision of a larger quantity of positively charged ions with the surface of the electrode, which results in an increase in the electrode's temperature and ultimately leads to the wearing away of the electrode material.

When the T_{on} increased from 800 µs to 1600 µs, while keeping the same pulse current value, higher rates of increasing the EWR were decreased. This is because a wider discharge channel reduces the discharge energy density and plasma cleansing efficiency, resulting in a decrease in EWR. This is illustrated in Fig. 3(d). The reason is that vegetable oil contains fewer carbon atoms than other dielectrics. The EWR value peaked at 2.573 mm³/min, with the highest values of I_P (30 A) and T_{on} (1600 µs).

Fig. 3(e) depicts the correlation among the current (I_P), pulse-on-times (T_{on}), and SR. Observations indicate that increasing the current (I_P) from 10 A to 30 A leads to a 17.28% rise in

the SR. Similarly, maintaining the same pulse-on-times of 800 and 1600 µs resulted in an 8.57% increase in SR, respectively. Increasing the pulse duration (T_{on}) to 800 µs and 1600 µs led to a slight rise in SR. More precisely, the SR had a 13.39% rise when a pulse current of 10 A was applied. Similarly, when a pulse current of 30 A was used, the SR increased by 4.97%. These results are shown in Fig. 3(f). The surface roughness deteriorated with the increase in pulse current. This is because of the increase in the electrical current, which led to a greater release of energy and force. The reason for this is that vegetable oil has fewer carbon atoms than other dielectrics. Consequently, a greater amount of melted material was removed, leading to the formation of deeper and larger discharge craters. Therefore, the surface roughness increases. The relationship between SR and T_{on} is directly proportional. As T_{on} increases, there is a corresponding increase in the discharge energy and the period over which this energy is discharged to the workpiece. This phenomenon causes the creation of bigger craters on the workpiece, leading to an augmentation in surface roughness, as depicted in Fig. 3(f).

3.2. Impact of input parameter on MRR, EWR, and SR for PMND-EDM

The PMND-EDM investigations conducted involved the utilization of kaolinite $Al_2SiO_2(OH)_4$ nanoparticles as additives, in combination with various gases (air, Ar, mix, and Ferron), in the vegetable oil dielectric. These experiments were carried out at varied operating pressures. The workpiece Al7075/NCGP samples were machined according to the specified experimental conditions. Tables 9-12 display the performance results for wet-EDM, ND-EDM, and PMND-EDM.

Table 8. Results of the wet-EDM response performance when using vegetable oil as a dielectric material.

Input parameters			Output parameters				
No.	Ip (Amp)	T_{on} (µs)	MRR (g/min)	MRR (mm^3/min)	EWR (g/min)	EWR (mm^3/min)	SR (µm)
1	10	800	0.0128	4.604	1.66×10^{-3}	0.186	5.475
2	10	1600	0.0146	5.252	0.0117	1.309	6.208
3	30	800	0.0941	33.849	0.0180	2.013	6.421
4	30	1600	0.0990	35.612	0.0230	2.573	6.740

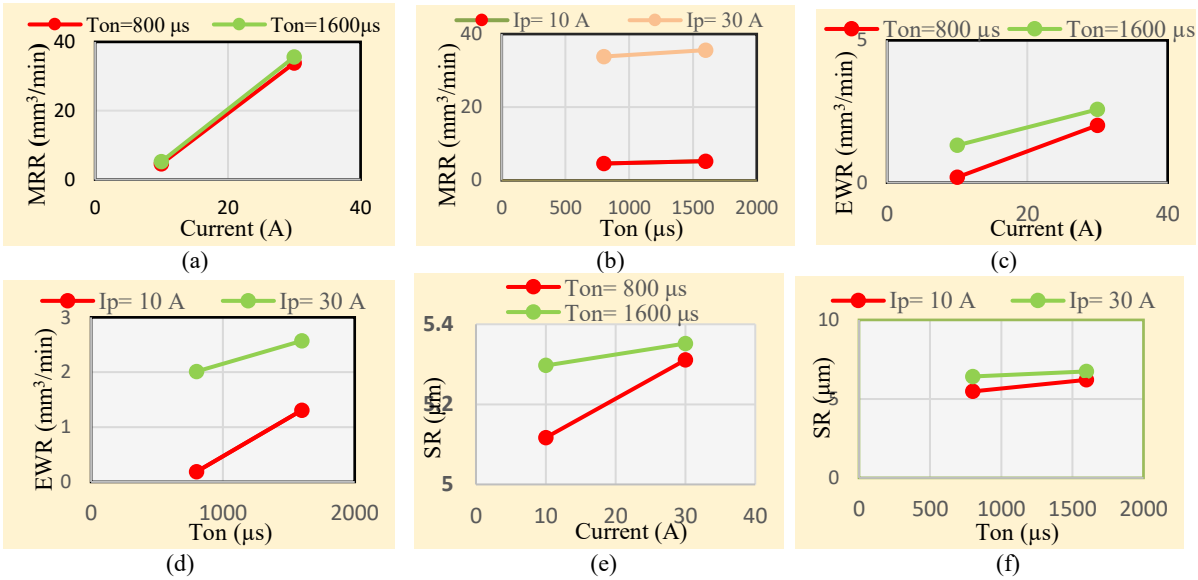

Fig. 3. (a) The influence of I_P at constant Ton, (b) the effect of Ton on MRR at constant I_P, (c) the effect of T_{on} on EWR at constant I_P, (d) the effect of Ip on EWR at constant T_{on}, (e) the effect of T_{on} on SR at constant Ip, (f) the effect of Ip on SR at constant T_{on} and (f) SR for wet-EDM experiments.

Table 9. The response data for NDEDM and PMND-EDM (vegetable oil+ air+ kaolinite $Al_2SiO_2(OH)_4$).

Input parameters				Output parameters				
No.	Ip Amp	T_{on} µs	PC %	MRR g/min	MRR mm^3/min	EWR g/min	EWR mm^3/min	SR µm
1	10	800	0%	9.176×10^{-3}	3.301	9.647×10^{-3}	1.079	5.117
2	10	1600	0%	0.0105	3.777	8.609×10^{-3}	0.972	5.297
3	30	800	0%	0.0556	20.068	3.092×10^{-3}	0.346	5.311
4	30	1600	0%	0.0749	26.943	4.059×10^{-3}	0.454	5.352
5	10	800	5%	2.99×10^{-3}	1.076	4.58×10^{-4}	0.051	5.510
6	10	1600	5%	1.928×10^{-3}	0.694	1.24×10^{-3}	0.139	6.003
7	30	800	5%	0.021	7.554	9.655×10^{-4}	0.108	7.371
8	30	1600	5%	0.0428	15.396	6.66×10^{-4}	0.075	8.085
9	10	800	10%	1.951×10^{-3}	0.702	2.623×10^{-4}	0.029	4.541
10	10	1600	10%	1.924×10^{-3}	0.692	7.868×10^{-3}	0.880	4.796
11	30	800	10%	0.011	3.957	1.789×10^{-4}	0.020	6.862
12	30	1600	10%	0.021	7.554	2.601×10^{-4}	0.029	6.813

Table 10. The NDEDM and PMND-EDM (vegetable oil + Ar + kaolinite $Al_2SiO_2(OH)_4$) response date.

Input parameters				Output parameters				
No.	Ip Amp	T_{on} µs	PC %	MRR g/min	MRR mm^3/min	EWR g/min	EWR mm^3/min	SR µm
1	10	800	0%	4.062×10^{-3}	1.461	1.068×10^{-3}	0.120	4.761
2	10	1600	0%	7.160×10^{-3}	2.576	4.022×10^{-3}	0.450	5.287
3	30	800	0%	0.0392	14.101	3.75×10^{-3}	0.420	5.937
4	30	1600	0%	0.025	8.993	9.677×10^{-3}	1.082	6.276
5	10	800	5%	6.66×10^{-3}	2.396	1.699×10^{-3}	0.190	5.135
6	10	1600	5%	8.017×10^{-3}	2.884	2.758×10^{-3}	0.309	5.362
7	30	800	5%	0.044	15.827	2.985×10^{-3}	0.334	6.805
8	30	1600	5%	0.026	9.353	3×10^{-3}	0.336	7.241
9	10	800	10%	2.47×10^{-3}	0.889	2.022×10^{-4}	0.023	3.943
10	10	1600	10%	3.180×10^{-3}	1.144	7.228×10^{-5}	0.008	5.217
11	30	800	10%	0.039	14.029	3.55×10^{-3}	0.397	6.528
12	30	1600	10%	0.040	14.389	7.739×10^{-4}	0.087	6.913

Table 11. Results of responses for NDEDM and PMND-EDM (vegetable oil plus mix (Ar + N_2) + kaolinite $Al_2SiO_2(OH)_4$).

Input parameters				Output parameters				
No.	Ip Amp	T_{on} µs	PC %	MRR g/min	MRR mm^3/min	EWR g/min	EWR mm^3/min	SR µm
1	10	800	0%	8.137×10^{-3}	2.927	2.712×10^{-3}	0.303	4.567
2	10	1600	0%	8.7×10^{-3}	3.130	2.3×10^{-3}	0.257	4.634
3	30	800	0%	0.0556	20.000	1.568×10^{-3}	0.175	5.461
4	30	1600	0%	0.0818	29.425	6.9767×10^{-3}	0.780	6.341
5	10	800	5%	2.015×10^{-3}	0.725	2.344×10^{-5}	0.003	4.797
6	10	1600	5%	5.601×10^{-3}	2.015	4.552×10^{-4}	0.051	4.891
7	30	800	5%	0.043	15.468	4.587×10^{-4}	0.51	6.021
8	30	1600	5%	0.038	13.669	1.247×10^{-3}	0.140	5.863
9	10	800	10%	3.205×10^{-3}	1.153	2.158×10^{-4}	0.024	4.987
10	10	1600	10%	5.64×10^{-3}	2.029	8×10^{-5}	0.009	6.585
11	30	800	10%	0.0206	7.410	7.575×10^{-5}	0.009	6.763
12	30	1600	10%	0.033	11.871	1.45×10^{-3}	0.162	6.963

Table 12. The findings for NDEDM and PMND-EDM (kaolinite Al2SiO2(OH)4, vegetable oil, and Freon gas).

Input parameters				Output parameters				
No.	Ip Amp	T_{on} µs	PC %	MRR g/min	MRR mm^3/min	EWR g/min	EWR mm^3/min	SR µm
1	10	800	0%	9×10^{-3}	3.237	1×10^{-4}	1.119	3.814
2	10	1600	0%	4.130×10^{-3}	1.486	1.304×10^{-4}	1.459	5.561
3	30	800	0%	0.049	17.626	3.703×10^{-4}	4.142	6.012
4	30	1600	0%	0.046	16.547	2.2×10^{-4}	2.461	6.812
5	10	800	5%	7.387×10^{-3}	2.657	1.814×10^{-3}	0.203	4.617
6	10	1600	5%	9.818×10^{-3}	3.532	0.0105	1.175	5.497
7	30	800	5%	0.0549	19.748	3.098×10^{-3}	0.347	7.421
8	30	1600	5%	0.063	22.662	7.246×10^{-3}	0.811	7.348
9	10	800	10%	4.186×10^{-3}	1.506	9.767×10^{-4}	0.109	4.756
10	10	1600	10%	0.0123	4.425	2.192×10^{-3}	0.245	5.646
11	30	800	10%	0.0298	10.719	6.185×10^{-4}	0.069	6.961
12	30	1600	10%	0.016	5.755	6.2614	0.700	7.835

These tables record the results of using different types of EDM process experiments using air, argon, a mixture of argon and nitrogen, and Freon, respectively. The abbreviation PC refers to the kaolinite $Al_2SiO_2(OH)_4$ nano powder concentration added to the vegetable oil dielectric. Comparative graphs illustrating the MRR were plotted and can be seen in Figs. 4 and 5.

The utilization of $Al_2SiO_2(OH)_4$ nanopowders as an additive, in combination with vegetable oil and air dielectric gas, demonstrated superior performance in terms of increased erosion rate. The rise in powder concentration (Cp) is directly related to the MRR. The likely explanation is that the powder possesses more hardness and thermal conductivity. The conductive powder particles arrange themselves in a chain-like arrangement, resulting in a bridging effect at the IEG or machining gap.

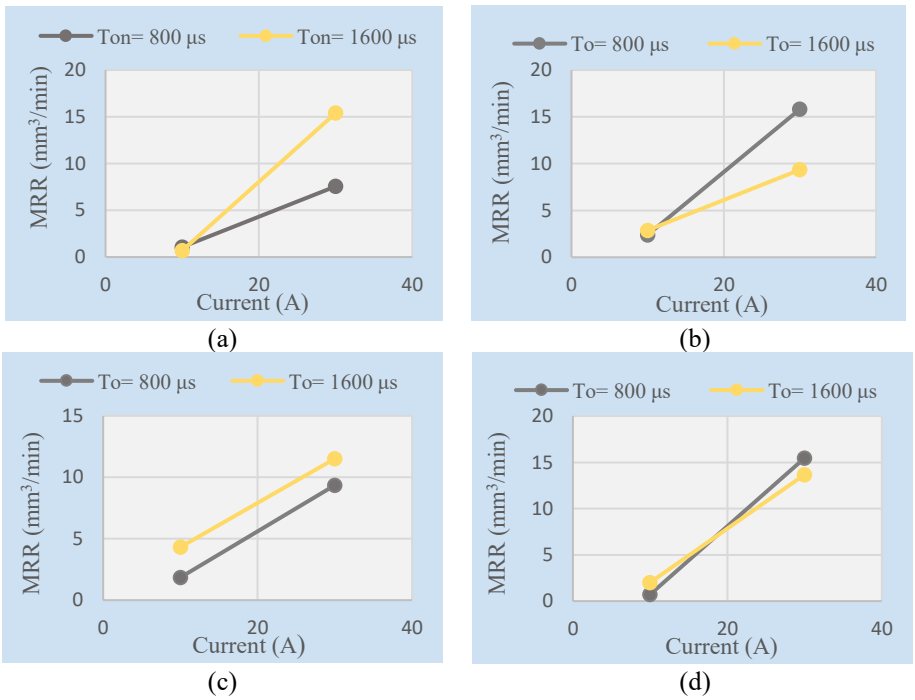

Fig. 4. The impact of I_P on MRR at constant T_{on} (PMND-EDM) using a vegetable oil dielectric and the additive nanopowders kaolinite $Al_2SiO_2(OH)_4$) with (a) air, (b) Ar,(c) mixed Ar+N_2, and (d) Freon.

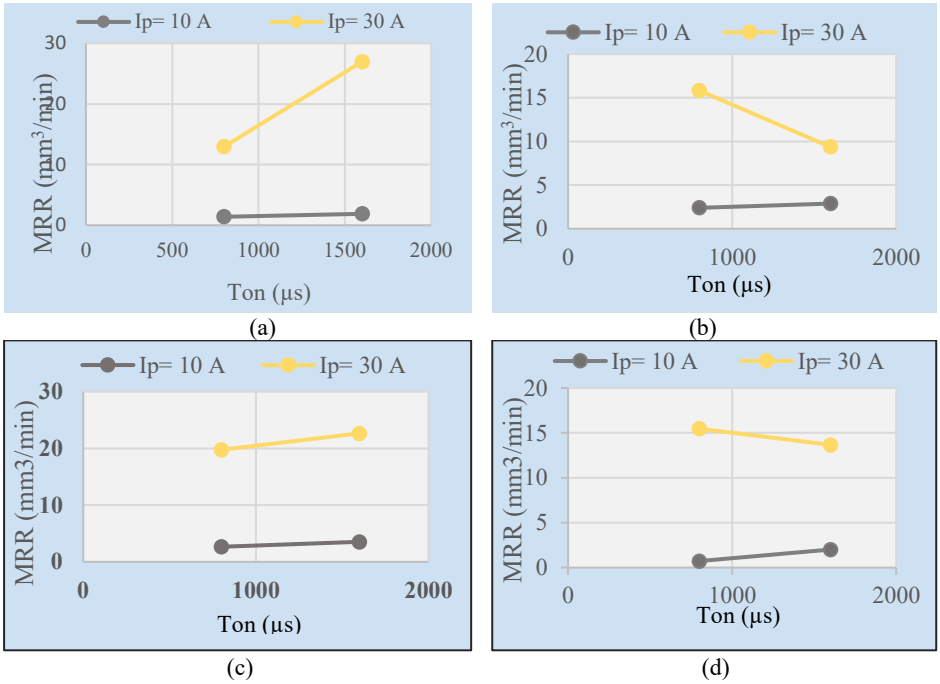

Fig. 5. The impact of Ip on MRR in ND-EDM at constant T_{on} using a a dry dielectric of (a) air, (b) Ar, (c) mixed Ar+N_2, and (d) Freon.

The bridging effect leads to an increase in the thermal conductivity of the dielectric medium between the electrodes. This results in a higher frequency of sparks and a more energetic plasma, ultimately leading to an enhanced erosion rate from the workpiece [39-41]. Additionally, the $Al_2SiO_2(OH)_4$ additive possesses a very low density, allowing the grain particles of $Al_2SiO_2(OH)_4$ to scatter evenly in the dielectric medium. This, in turn, creates favorable circumstances for erosion during machining. The addition of $Al_2SiO_2(OH)_4$ powder, in combination with dielectric gas, leads to a drop in MRR. This decrease may be attributed to short-circuiting caused by increasing powder density [42, 43].

The PMND-EDM investigations involved the utilization of specific nano additive powders, namely kaolinite ($Al_2SiO_2(OH)_4$, in conjunction with various gases (air, Ar, mix Ar+N_2, and Ferron). These tests were conducted under varied operating pressures while also incorporating the presence of vegetable oil.

Fig. 4 demonstrates the impact of discharge current on EWR, whereas Fig. 5 illustrates the influence of pulse-on-time on EWR. The EWR falls as the concentration of nanoparticles (% Cp) increases.

With different dielectrics, such as vegetable oil alone, + Air + 0%, 5%, and 10% $Al_2SiO_2(OH)_4$, the lowest achieved EWR was obtained using the input parameters Ip (10, 30 A) and T_{on} (800, 1600 µs). The EWR values reached 0.972 (when using 1600 µs and 10A), 0.051 (when using 800 µs and 10A), and 0.020 mm^3/min (when using 800 µs and 30A), as shown in Figs. 6 and 7. The recorded EWR values are much lower than the minimum value obtained when using vegetable oil alone or as a dielectric under the same machining conditions, with differences of 422.59% (highest), 264.71%, and 830.00%, respectively. The lowest achieved EWR, using the same dielectrics but substituting air with Ar additive gas, was 0.120 (800 µs, 10A), 0.190 (800 µs, 10A), and 0.008 mm^3/min (1600 µs, 10A), respectively.

The EWR values obtained are significantly lower than the lowest value achieved when using vegetable oil alone or as a dielectric under the same machining circumstances. The reduction in EWR is 55.00, 2.15 (higher), and 2225.00%, respectively.

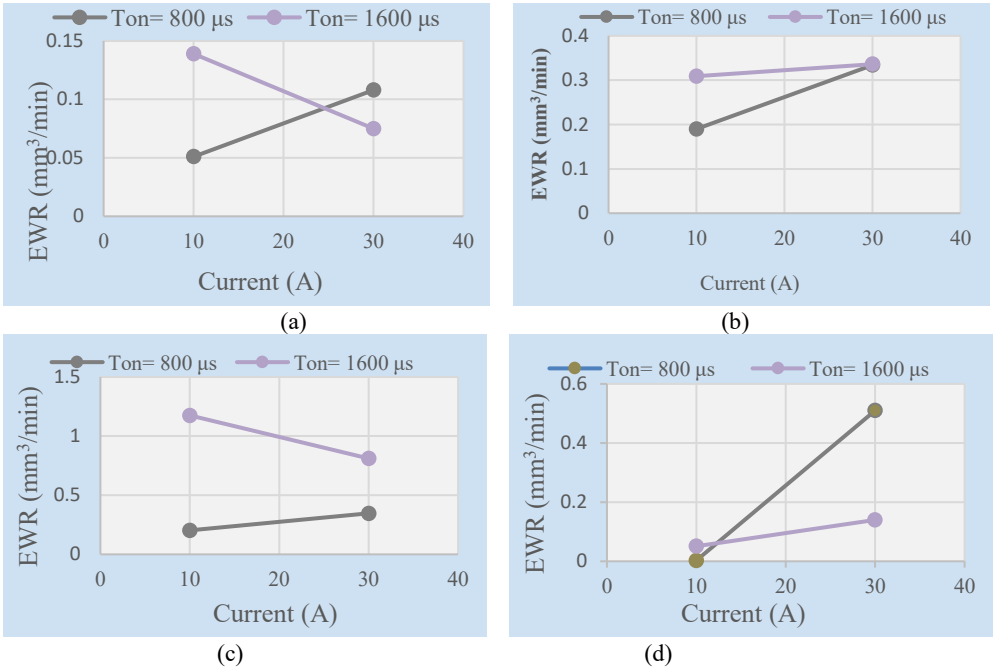

Fig. 6. The impact of I_P on EWR at constant T_{on} (PMND-EDM) using a vegetable oil dielectric and the additive nanopowders kaolinite $Al_2SiO_2(OH)_4$) with (a) air, (b) Ar, (c) mixed Ar+N_2, and (d) Freon.

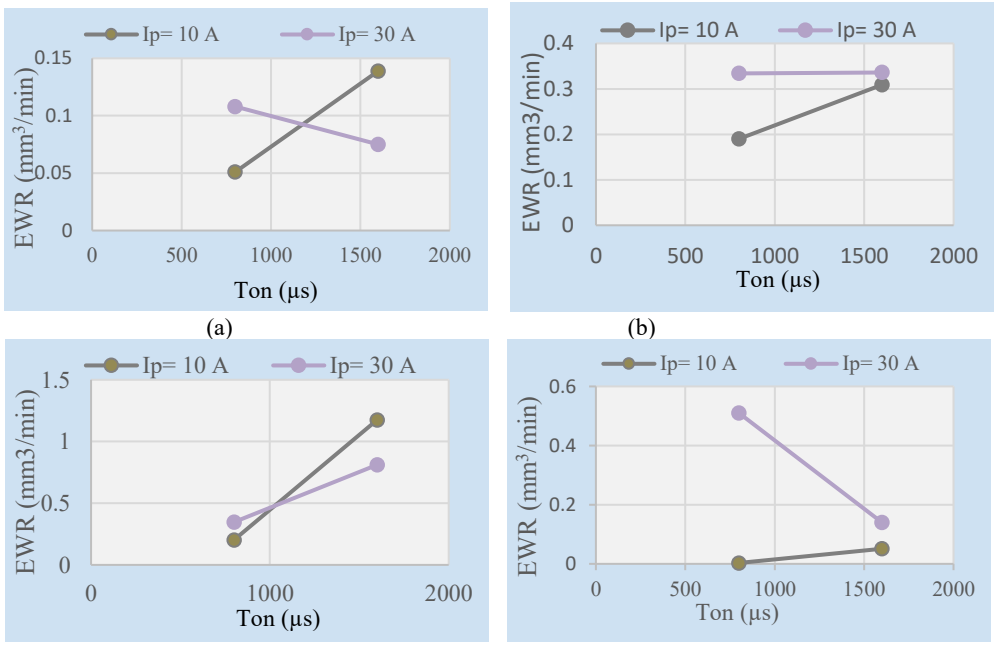

Fig. 7. The impact of T_{on} on EWR at constant Ip (PMND-EDM) using a vegetable oil dielectric and the additive nanopowders kaolinite $Al_2SiO_2(OH)_4$) with (a) air, (b) Ar, (c) mixed Ar+N_2, and (d) Freon.

The lowest achieved EWR using the identical dielectrics but substituting air with a Freon additive gas as the dielectric was 0.175 mm^3/min (at 800 µs and 30A), 0.003 mm^3/min (at 800 µs and 10A), and 0.009 mm3/min (at 1600 µs and 10A or 800 µs and 30A), respectively. The values of EWR acquired are much lower than the minimum value obtained when using vegetable oil alone as a dielectric under the same machining conditions. The reduction in EWR is

9.29%, 6100.00%, and 66.67%, respectively. The nano additive powder particles form a bridge-like structure in the inter-electrode gap (IEG), causing the machining gap to widen. The extended IEG enhances the plasma channel, hence decreasing the likelihood of short-circuiting between the tool and workpiece electrodes [44, 45].

This phenomenon, characterized by a decrease in heat transmission, causes the temperature of the materials to fall below their melting point, resulting in a reduction in the Electrode Wear Rate (EWR). Moreover, the inclusion of metallic powder additions decreases the breakdown voltage. It increases the gap between electrodes, enhancing the overall stability of the machining process and further reducing the EWR. However, introducing $Al_2SiO_2(OH)_4$ powder, Ar gas, and Ferron gas at an Ip of 30A and Ton of 800 µs increased the EWR.

This phenomenon can be attributed to the reduction in gap voltage and insulation strength of the medium when $Al_2SiO_2(OH)_4$ is introduced. A short circuit in the gap leads to an early explosion due to high EWR. Both used nanopowders share the same cause. The lowest equivalent weight retention (EWR) at the initial potential (I_P) of 10A, the pulse duration (T_{on}) of 1600 µs, and the duty cycle (Cp) of 5% were attained while using a combination of vegetable oil and Freon.

The PMND-EDM experiments used kaolinite nanoparticles as additives, along with different mixing gases (air, Ar, mix (Ar+N_2), and Freon). Vegetable oil was also used as a dielectric. The findings show that the SR values for PMND-EDM increased when the discharge current was raised from 10 A to 30 A while keeping the pulse at times constant at 800 and 1600 µs. This is illustrated in Figs. 8 and 9.

The lowest achievable SR was 5.117 µm when utilizing the additive air-gas to dielectric. This was accomplished with a current of 10A and a ton of 800 µs. Another experiment using 5% $Al_2SiO_2(OH)_4$ resulted in a surface roughness of 5.510 µm, while using 10% $Al_2SiO_2(OH)_4$ resulted in a surface roughness of 4.541 µm. The obtained values of SR are 7.00, 0.64 (higher), and 20.57% lower than the lowest value achieved when using vegetable oil alone, respectively.

The lowest achievable SR was 3.287 µm when using vegetable oil and the additive Ar gas as a dielectric. This was accomplished with a current of 10A, a pulse duration of 1600 µs, and no percentage of nanopowder concentration (C_p). Another experiment using the same parameters but with 5% Cp of $Al_2SiO_2(OH)_4$ resulted in a surface roughness of 5.135 µm. Lastly, when 10% C_p of $Al_2SiO_2(OH)_4$ was used, the surface roughness was measured at 3.943 µm. The obtained values of SR are 66.67%, 6.62%, and 38.71% lower than the lowest value achieved when using vegetable oil alone, respectively.

The lowest attainable SR utilizing a mixture of Ar and N_2 gases as a dielectric was 3.814 µm. This was achieved by employing a current of 10A, a pulse duration (T_{on}) of 800 µs, and a mixture of vegetable oil with 0% C_p. Additionally, surface roughness values of 4.617 µm and 4.756 µm were obtained using 5% and 10% Cp $Al_2SiO_2(OH)_4$, respectively.

The obtained values of SR are 43.55%, 18.58%, and 15.12% lower than the lowest value achieved when using vegetable oil alone, respectively. The lowest achieved SR using the same dielectrics but substituting air with Freon as the dielectric and employing a 10A, T_{on} (800 µs) pulse with a mixture of vegetable oil, Ferroin, and 0% Cp was 4.567 µm. When using the same parameters but with a 5% Cp additive, the SR improved to 4.797 µm. Finally, by increasing the Cp $Al_2SiO_2(OH)_4$ concentration to 10%, the SR further improved to 4.987 µm.

The measured SR values are 19.88%, 14.13%, and 9.79% below the minimum value obtained when using vegetable oil alone, respectively. The results' analysis showed that pulse current and pulse on time were the two most important process parameters for SR in PMND-EDM.

Figs. 8 and 9 demonstrate that the SR rises as the discharge current and pulse-on-time increase. The cause is the same as that of the parameters mentioned in the previous response.

The use of nanoparticles as additives in the dielectric has resulted in a small improvement in the SR when compared to the achieved MRR. Powder particles cause the plasma formed between the electrodes to increase in size.

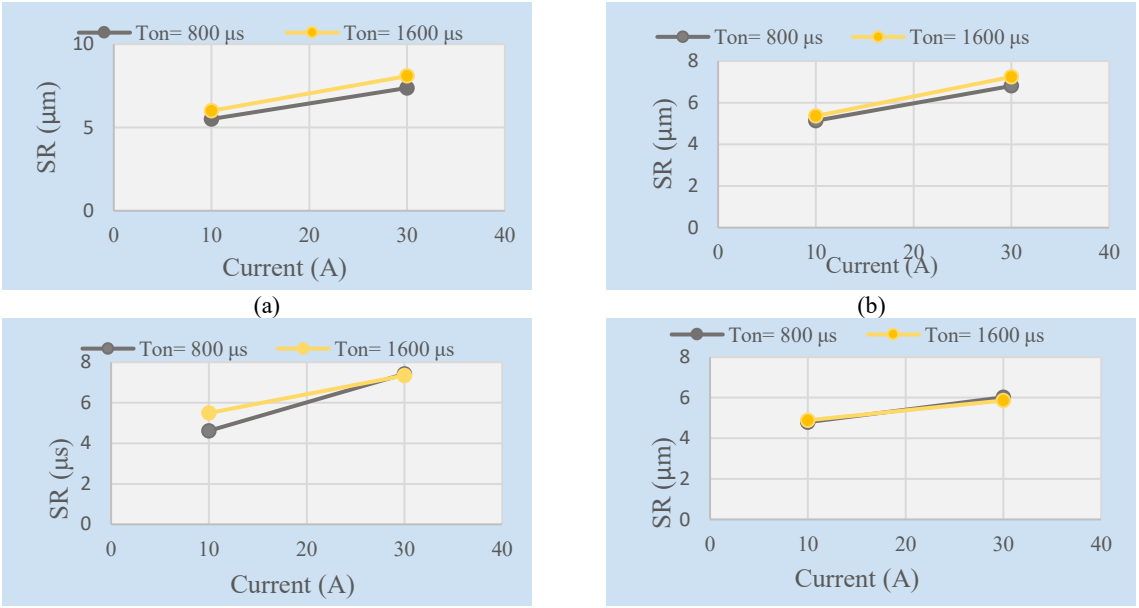

Fig. 8. The impact of I_P on SR at constant T_{on} (PMND-EDM) experiments using a vegetable oil dielectric and %5 additive nanopowders kaolinite $Al_2SiO_2(OH)_4$) with (a) air, (b) Ar, (c) mixed Ar+N_2, and (d) Freon.

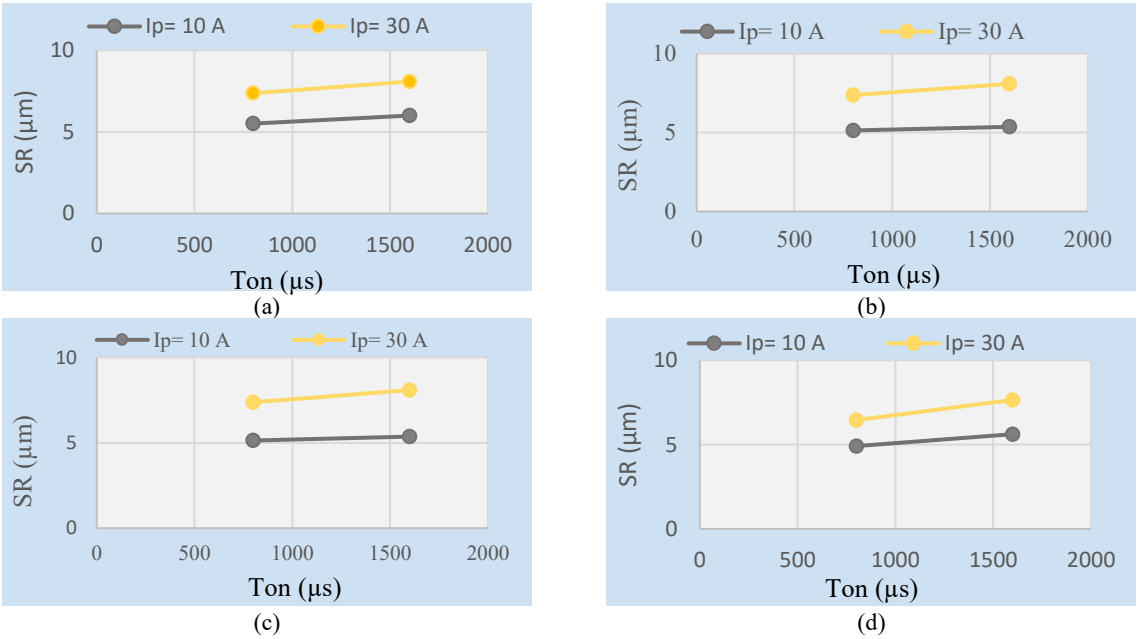

Fig. 9. The impact of T_{on} on SR at constant Ip (PMND-EDM experiments using a vegetable oil dielectric and %5 additive nanopowders kaolinite $Al_2SiO_2(OH)_4$) with (a) air, (b) Ar, (c) mixed Ar+N_2, and (d) Freon.

The discharge energy of the many sparks is uniformly dispersed across a broader surface area [46]. Furthermore, the molten metal in the machining gap experienced less compression from the gas bubbles and plasma channel, resulting in a surface that is less concave and consistently smooth [47]. The high density of Cp $Al_2SiO_2(OH)_4$ prevents particles from uniformly mixing with the dielectric. Furthermore, upon their addition to the dielectric, powder particles agglomerate due to either the Van der Waals forces or electrostatic forces. Hence, an excessively high concentration of powder particles leads to short-circuiting and incorrect

discharges, resulting in the degradation of the surface finish of the machined samples. Based on the information provided, it may be inferred that the sedimentation rate (SR) is inversely related to the concentration of Cp.

3.3. The resulting white recast layer's response of wet-EDM, ND-EDM, and PMND-EDM parameters.

A thin, white layer known as the "recast layer" develops during EDM processes on the workpiece's machined surface. It forms when the liquid material cools and hardens and is then deposited on the machined surface. The recast layer is created when the dielectric fluid fails to entirely remove molten material from the IEG [48, 49]. The transformation of the work material's metallurgical properties due to the presence of a rigid and fragile layer can lead to severe and potentially disastrous failure [50, 51]. Therefore, to examine the impact of various dielectric mediums on surface topology, we analyzed representative machined surfaces to determine the thickness of the recast layer under increasing discharge energy levels.

The SEM analysis showed that the average thickness of the recast white layer formed by wet-EDM (using vegetable oil only) was 3.133 µm at an I_P of 30A and a Ton of 1600 µs, as shown in Fig. 10. In the ND-EDM, the average thickness of the recast white layer was 1.505 µm for vegetable oil + air, 1.180 µm for vegetable oil + Ar, 0.456 µm for vegetable oil + mix (Ar-N_2), and 0.000 µm for vegetable oil + Ferron. On the other hand, in the case of PMND-EDM, when $Al_2SiO_2(OH)_4$ powder was added, the thicknesses were 0.886 µm, 0.833 µm, 1.036 µm, and 0.000 µm, respectively, as shown in Fig. 11.

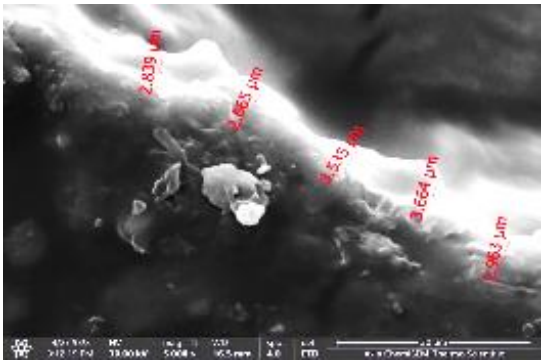

Fig. 10. SEM analysis of recast white layer thickness during wet-EDM experiments at I_p (30A) and T_{on} (1600 µs).

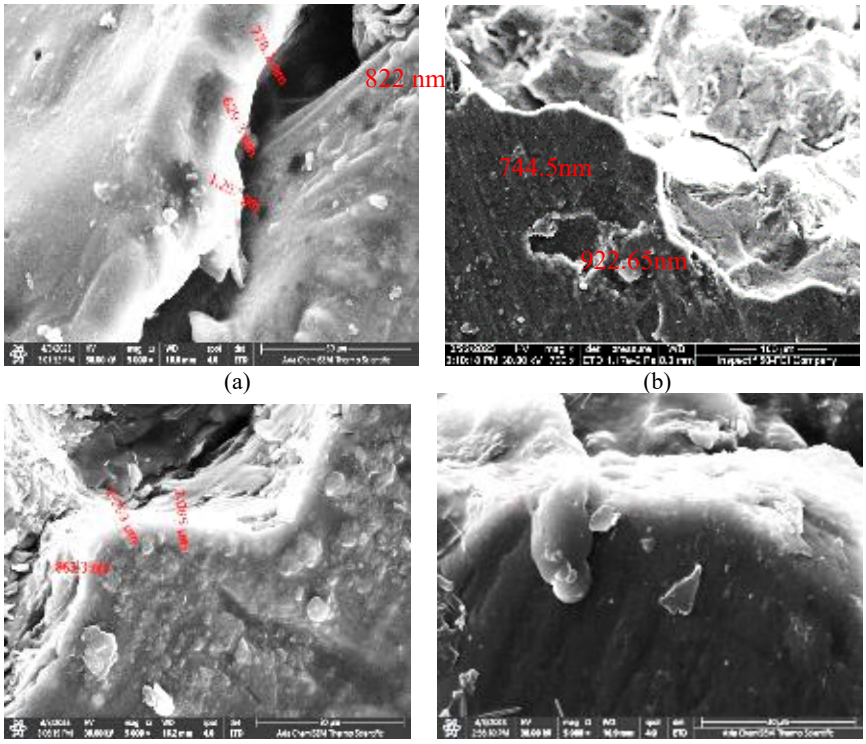

(a) (b)

(c) (d)

Fig. 11. SEM analysis of the recast white layer thickness for PMND-EDM at I_p (30A), T_{on} (1600 µs), using a vegetable oil dielectric and 10% C_p of ($Al_2SiO_2(OH)_4$) with (a) air, (b)Ar ,(c) mix, and (d) Freon.

The use of Ferron as a gas, whether in ND-EDM or PMND-EDM, did not result in any detectable recast layer thicknesses. However, when vegetable oil is combined with either Freon or Ferron and nano powder to create a dielectric medium, it leads to an explosive reaction between the IEG. This reaction disperses debris from the IEG, thereby enhancing the flushing efficiency in the gap and effectively preventing debris deposition on the machined surface.

The prior traditional EDM process, using a pulse current of 15 A, formed a thick, re-solidified white layer measuring 31.34 µm [37].

Nevertheless, in the current study, the highest thickness of the recast layer was determined to be 3.133 µm using wet-EDM with vegetable oil as the dielectric medium. Generally, the ND-EDM and PMND-EDM processes resulted in thinner recast layers compared to the conventional wet-EDM process when operating at I_p (30A) and T_{on} (1600 µs).

The reduction in thickness was 108.17%, 165.51%, 630.26%, and (∞) when using air, Ar, mix (Ar-N_2), and Freon gases in combination with vegetable oil dielectrics for ND-EDM. For PMND-EDM, the reduction was 253.61%, 276.11%, 202.41%, and (∞) when using the same gases along with $Al_2SiO_2(OH)_4$ powder.

These novel findings can extend the service and fatigue lives of machines and parts subjected to sudden dynamic mechanical or thermal loads without requiring additional procedures to remove the brittle layer, which contributes to the failure of parts with short service lives.

3.4. Evaluation of PMND-EDM machining performance against wet and ND-EDM

Fig. 12(a) displays the highest MRR values achieved after conducting all the planned experiments. Fig. 12(a) compares the MRR produced from wet-EDM, ND-EDM, and PMND-EDM. The PMND-EDM process achieved the highest Material Removal Rate (MRR) values when using higher discharge energy levels (I_p=30, T_{on}= 1600µs, and C_p=10%). The rise in MRR can be due to the higher oxygen content in the air, which leads to a more exothermic reaction and generates additional heat. The oxidation process is attributed to these exothermic processes [52].

Another contributing factor to this phenomenon is that oxygen has a comparatively lower ionization energy than other gases. The gas with lower ionization energy has a propensity to undergo ionization at a faster rate, leading to a higher achieved MRR [53]. Because of the high ionization potential of oxygen gas, the oxygen atom readily acquires electrons and forms compounds with positive ions. The simple process of deionization causes a consistent discharge in the case of oxygen-assisted EDM, resulting in an increase in MRR [54].

Fig. 12(a) displays the highest Material Removal Rate (MRR) values achieved after conducting all the planned experiments. Fig. 12(b) compares the Electrode Wear Ratio (EWR) results for wet-EDM, ND-EDM, and PMND-EDM. At higher levels of discharge energy, specifically with an input power (I_p) of 30A, a pulse duration (T_{on}) of 1600 µs, and a capacitance (Cp) of 10%, the EWR in PMND-EDM was significantly lower compared to wet-EDM and ND-EDM. This is because the additive nanopowder particles form a bridge-like structure at the IEG, thereby increasing the machining gap. Furthermore, the EWR obtained using only vegetable oil as the dielectric medium was approximately three times higher than the EWR obtained using other investigated dielectric mediums.

The highest attainable MRR, influenced by the input parameters I_P (30A), T_{on} (1600 µs), and the utilization of a mixture of vegetable oil and air, achieved values of 26.943 mm^3/min (with 0% C_p), 15.396 mm^3/min (with 5% $Al_2SiO_2(OH)_4$), and 7.554 mm^3/min (with 10% additive nanopowder, as seen in Figs. 3 and 4.

The MRR values obtained are 32.17%, 131.33%, and 2861.20%, lower than the maximum values produced when using vegetable oil alone as a dielectric under the same machining conditions. The MRR achieved using the same dielectrics as mentioned above, but substituting air with Ar additive gas, reached 14.101 (using 800 µs, 0% C_p) and 15.827 (using 800 µs, and 5% $Al_2SiO_2(OH)_4$), and 14.389 mm^3/min (using 10% $Al_2SiO_2(OH)_4$), respectively. These MRR values are 152.55%, 125.01%, and 147.50%, higher than the highest values obtained when using vegetable oil alone as a dielectric.

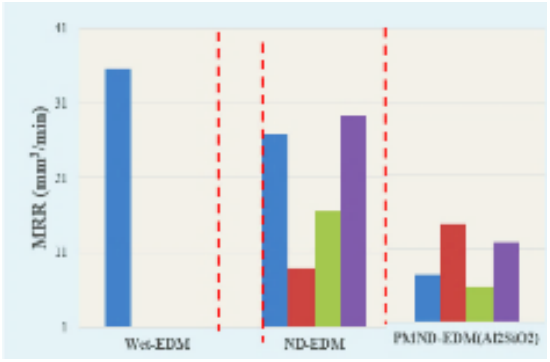

(a)

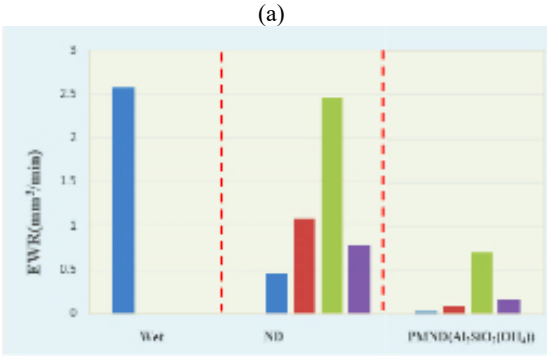

(b)

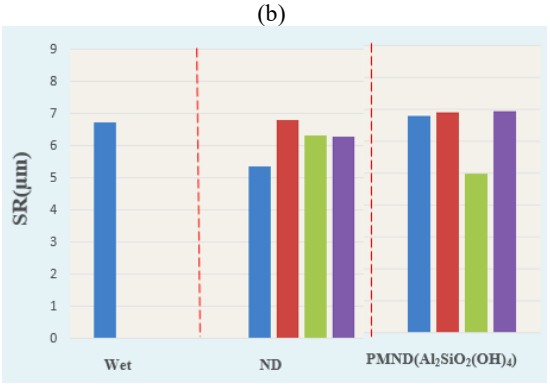

(c)

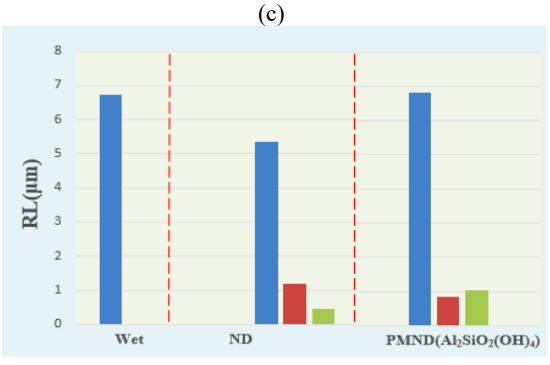

(d)

Fig. 12. The results are in comparison of wet-EDM, ND-EDM, and PMND-EDM; (a) MRR; (b) EWR; (c) SR; (d) WLT, using a vegetable oil dielectric and 0-10% C_p of ($Al_2SiO_2(OH)_4$) with air (blue color); Ar (red color), mix (green color), and Freon (purple color).

The maximum attainable MRR attained with the combination of Ar and N_2 gases as additives to the dielectric was 17.626 (with a pulse duration of 800 µs and 0% C_p), 22.662 (with 5% $Al_2SiO_2(OH)_4$), and 10.719 mm^3/min (with a pulse duration of 800 µs and 10% $Al_2SiO_2(OH)_4$), respectively. The MRR values obtained when utilizing vegetable oil alone as a dielectric are 102.04%, 191.19%, and 57.14% higher than the obtained values.

The maximum attainable MRR utilizing the Freon additive gas was 29.425 (with 0% C_p), 15.468 (with 800 µs and 5%, and 11.871 mm^3/min (with 10% $Al_2SiO_2(OH)_4$), respectively. The MRR values produced when using vegetable oil alone are 21.03%, 130.23%, and 199.99% higher than the obtained values.

Fig. 12(b) demonstrates that the lowest EWR values achieved in all the experiments conducted were 0.003 mm^3/min. These values were obtained using the following conditions: I_p (10A), T_{on} (1600 µs), and a dielectric of vegetable oil+ Fr+ (5%) C_p $Al_2SiO_2(OH)_4$. The EWR values were increased to 0.008 and 0.009 mm^3/min when using I_p (10A), T_{on} (1600 µs), and vegetable oil+ Ar+ (10% C_p) $Al_2SiO_2(OH)_4$, and I_p (10 or 30A), T_{on} (800 or 1600 µs) with vegetable oil+ Fr+ (10% C_p) +$Al_2SiO_2(OH)_4$, respectively.

The lowest achieved EWR using the identical dielectrics, but with the addition of a mixture of Ar) and N_2 gases instead of air, was 1.119 mm^3/min (using 800 µs, 10A), 0.203 mm3/min (using 800 µs, 10A), and 0.069 mm3/min (using 800 µs, 30A), respectively. The EWR values obtained are 501.61% higher than the lowest value achieved when using vegetable oil alone, 8.60% higher than the lowest value obtained when using vegetable oil as a dielectric under the same machining conditions, and 54.13% higher than the lowest value obtained when using vegetable oil as a dielectric with the same machining settings.

The SR is produced through the utilization of a blend of gases in vegetable oil. The $Al_2SiO_2(OH)_4$ dielectric medium had a more refined texture in comparison to the other dielectric media investigated, as illustrated in Fig. 12(c). This figure illustrates that the minimum SR values obtained in all the

performed trials were 3.287 µm. The result was achieved by utilizing an I_p of 10A, T_{on} of 1600 µs, Ar as an additive gas, and a Cp of 0%. The next lowest SR values were 3.621 µm (achieved with the same pulse current, Ton (800 µs), and 5% SiO2), 3.814 µm (achieved with 0% C_p), and 3.943 µm (achieved with Ton (800 µs) and 10% $Al_2SiO_2(OH)_4$), respectively.

Fig. 12(d) compares the thickness of the white recast layer (RL) obtained from wet-EDM, ND-EDM, and PMND-EDM. At higher levels of discharge energy, namely with I_p=30, T_{on}=1600µs, and C_p=10%, the thickness of the recast layer was determined to be negligible in vegetable oil-Freon (ND-EDM) and vegetable oil-Ferron- $Al_2SiO_2(OH)_4$ (PMND-EDM).

Additionally, no significant recast layer was seen. The explosive reaction between the IEG is caused by the use of vegetable oil-Ferron or vegetable oil-Ferron with nanopowder as a dielectric medium. This reaction effectively removes debris from the gap and enhances the flushing efficiency at IEG. As a result, it prevents debris deposition on the machined surface. The thickness of the RL when air is used as the dielectric medium in any manner is roughly four times greater compared to when other dielectric mediums are used, as illustrated in Fig. 12(d).

The current experimentation aims to develop statistical models for wet-EDM and ND-EDM. This involves using various dielectric mixtures and analyzing their effects through a full factorial design. The two chosen factors for the EDM experiments are the controllable variables that have a significant impact on process characterization. These factors include pulse current, with two levels of 10A and 30A, pulse-on-time, with two levels of 800µm and 1600µm, and the number of replicates. The experimental values were analyzed using the general full factorial design with a 95% confidence interval and the Minitab statistical software with the general linear model.

The regression coefficients were employed to construct the mathematical model and predict the process responses for PMND-EDM using the experimental results obtained from Table 9. Eqs. (1-3) depict the regression models in their initial state, which establish a relationship between the process parameters and the responses of MRR, EWR, and SR utilizing PMND-EDM (a combination of air, vegetable oil, and $Al_2SiO_2(OH)_4$) correspondingly.

A model test examines the significance of each term in the model as a whole, while a lack-of-fit test determines the significance of any omitted factors in the model. Backward elimination regression can be used to delete non-significant components from the models, resulting in the production of a better model [54]. The Model Summary offers statistical data that enables the comparison of the effectiveness of different models in fitting the data. The R-Square (R-Sq) value measures the amount of variation in the observed responses that the model can explain. It is commonly known as the coefficient of determination. The adjusted R-square, denoted as R-Sq (adj), quantifies the fraction of the variance in the dependent variable that can be accounted for by a modified R-value.

This modified R-value takes into consideration the number of terms in the model. The expected R-square (R-Sq (pred)) measures the model's capacity to predict future data with accuracy. A higher value of R-Square (R-Sq) and adjusted R-square (R-Sq (adj)) suggests a better fit.

Fig. 13(a) shows the normal probability plots for the residuals of MRR, while Fig. 13(b and c) for EWR and SR of PMND-EDM (air + vegetable oil + $Al_2SiO_2(OH)_4$), respectively.

MRR= 0.02846 - 0.01954 Ip + 0.01954 Ip + 0.02649 Cp - 0.00698 Cp - 0.01951Cp 0.02201Ip×Cp + 0.00952 Ip×Cp+ 0.01249 Ip×Cp + 0.02201 Ip×Cp- 0.00952 Ip×Cp - 0.01249 Ip×Cp (1)

EWR = 0.005450 - 0.001683 Ip + 0.001683 Ip - 0.001833 Ton+ 0.001833 Ton + 0.008125 Cp - 0.004550 Cp - 0.003575 Cp - 0.001033 Ip×Ton+ 0.001033 Ip×Ton + 0.001033 Ip×Ton- 0.001033 Ip×Ton- 0.005242 Ip×Cp + 0.001833 Ip×Cp+ 0.003408 Ip×Cp+ 0.005242 Ip×Cp - 0.001833 Ip×Cp - 0.003408 Ip×Cp- 0.001942 Ton×Cp+ 0.001833 Ton×Cp + 0.000108 Ton×Cp + 0.001942 Ton×Cp - 0.001833 Ton×Cp - 0.000108 Ton×Cp (2)

SR = 6.390 - 0.658 Ip+ 0.658 Ip - 0.180 Cp + 0.817 Cp - 0.638 Cp (3)

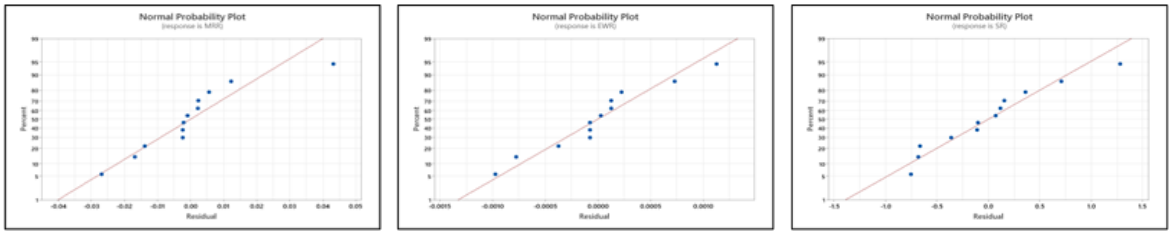

(a) (b) (c)

Fig.13. The residuals for PMND-EDM (air + vegetable oil + $Al_2SiO_2(OH)_4$); (a) for MRR, (b) EWR, and (c) SR, are plotted according to normal probability.

Table 13. Values of the output responded parameters for PMND-EDM with (air + vegetable oil + Al2SiO2(OH)4) predicted and experimented.

Run order	Exp. MRR (g/min)	Pred. MRR (g/min)	Residual value	Exp. EWR (g/min)	Pred. EWR (g/min)	Residual value	Exp. SR (µm)	Pred. SR (µm)	Residual value
1	0.0128	0.01340	-0.00060	0.0016	0.0018	-0.0002	5.475	5.552	-0.077
2	0.0146	0.01340	0.0006	0.0117	0.0114	0.0003	6.208	5.552	0.655
3	0.0941	0.0965	-0.00250	0.0180	0.0177	0.000	6.421	6.869	-0.448
4	0.099	0.0965	0.0025	0.023	0.023	0.000	6.740	6.869	-0.129
5	0.0029	0.01145	0.0095	0.0004	0.0004	0.0000	5.510	5.555	-0.035
6	0.0019	0.0114	- 0.0095	0.0012	0.0020	0.0000	6.003	6.549	-0.546
7	0.021	0.03150	-0.01050	0.0009	0.0000	0.0008	7.371	7.865	-0.494
8	0.0428	0.0315	0.0105	0.0006	0.0002	0.0004	8.085	7.865	0.219
9	0.0019	0.001	0.000	0.0002	0.0008	-0.0006	4.541	5.094	-0.553
10	0.0019	0.0019	-0.0000	0.0078	0.0063	-0.0000	4.796	5.094	-0.2988
11	0.011	0.01600	-0.00250	0.0001	0.0001	0.0000	6.862	6.411	0.450
12	0.021	0.0160	0.0050	0.0002	0.0008	-0.0006	6.813	6.411	0.4018

The data clearly exhibits an evident pattern, with the data points aligning linearly. These findings indicate that each component influences the MRR, EWR, and SR in the PMND-EDM while using the dielectric made of air, vegetable oil, and $Al_2SiO_2(OH)_4$. The results obtained from the regression model (which predicts values based on the full factorial design model) and the actual values obtained from experiments are presented in Table 13.

4. Conclusions

The following describes the primary conclusions of the current work:

1. The ND-EDM achieved a maximum MRR of 29.425 mm3/min using Vegetable oil + Freon gas as the dielectric. The obtained MRR when using vegetable oil alone is lower by 21.03%. During the PMND-EDM process, the maximum achieved MRR utilizing Freon gas was 15.468 (with a duration of 800 µs and 5% $Al_2SiO_2(OH)_4$).
2. In the near-dry EDM process, the lowest EWR was attained by employing Argon gas, resulting in a value of 0.120 mm^3/min. This value is 55.00% lower than that obtained when using vegetable oil alone. The minimum attainable EWR, using PMND-EDM and Freon gas, was 0.005 (at 1600 µs and 10A), whereas using vegetable oil + 5% and 10% $Al_2SiO_2(OH)_4$, the EWR values were 0.003 (at 800 µs and 10A) and 0.003, respectively.
3. The ND-EDM technique with a mixture of vegetable oil and inert gases (argon and nitrogen) achieved the lowest surface roughness of 3.814 µm. The resulting value of SR is 43.55% lower than the lowest value obtained when using vegetable oil alone.

Similarly, the minimum surface roughness obtained by using vegetable oil and argon gas was 3.943 µm (with a 10% concentration of Cp $Al_2SiO_2(OH)_4$). This value is 38.71% lower than the lowest SR obtained when using vegetable oil alone.

4. The SEM examination showed that the mean thickness of the recast white layer produced by wet-EDM (employing just vegetable oil) was 3.133 µm. The average thickness of the layers in the ND-EDM for the combinations of vegetable oil + air, vegetable oil + Ar, vegetable oil + mix (Ar-N2), and vegetable oil + Ferron were 1.505, 1.180, 0.456, and 0.000 µm, respectively. On the other hand, in the case of PMND-EDM with the addition of $Al_2SiO_2(OH)_4$ powder, the thicknesses produced were 0.886, 0.833, 1.036, and 0.000 µm, respectively.
5. It was discovered that the ND-EDM and PMND-EDM processes resulted in a thinner recast layer compared to the traditional wet-EDM process. The reduction in thickness was 108.17%, 165.51%, 630.26%, and (∞) when air, Ar, mix (Ar-N2), and Freon gases were added to the vegetable oil dielectrics for ND-EDM. For PMND-EDM, the reduction in thickness was 253.61%, 276.11%, 202.41%, and (∞) when the same gases were added along with $Al_2SiO_2(OH)_4$ powder.
6. The constructed mathematical models demonstrated a higher R-square and adjusted R-square value, indicating a superior level of correspondence. The normal probability plots of residuals for MRR, EWR, and SR displayed a distinct pattern, with the points aligning linearly. This pattern signifies that each factor influences the mentioned responses, as well as the outcomes derived from the regression model (predicted values) and the actual values obtained from experiments.

Acknowledgment

This research was not supported/partially by [Biomedical Engineering Department, University of Technology, Iraq], although they may not agree with all of the interpretations/conclusions of this paper.

References

[1] A. Pandey, S. Singh, "Current research trends in variants of electrical discharge machining: a review. *Int. J. of Eng. Sci. and Tech*. Vol. 2, pp. 2172-2191, (2010).

[2] W. Grzesik, "Advanced machining processes of metallic materials: theory, modeling, and applications" *Elsevier*, (2008).

[3] M. P. Groover, Fundamentals of modern manufacturing: materials processes, and systems. *John Wiley & Sons*, (2007).

[4] S. M. Ali "Influence of electrodes and parameters on micro-edm drilling performances of 304l stainless steel" 2nd International Conference on Engineering Technology and its Applications (IICETA), Al-Najef, Iraq, pp. 55-60, (2019).

[5] S. Paramashivan, J. Mathew, S. Mahadevan, "Mathematical modeling of aerosol emission from die-sinking electrical discharge machining process", *Appl. Math. Modell.,* Vol. 36, pp. 1493-1503, (2012).

[6] A. Abrol, V. K. Singla, "Study on optimization and machining characteristics of electric discharge machining using powder suspension dielectric fluids", *A thesis*, Thapar University, (2012).

[7] N. A. Abukhshim, P. T. Mativenga, M. A. Sheikh, "Heat generation and temperature prediction in metal cutting: a review and implications for high-speed machining" *Int. J. Mach. Tools Manuf.*, Vol. 46, pp. 782-800, (2006).

[8] A. Al-Khazraji, S. Amin and S. M. Ali "The effect of sic powder mixing electrical discharge machining (PMEDM) on fatigue life of aisi d2 die steel", *Eng. Sci. Technol. Int. J.*, Vol.19, pp. 1400-1415, (2016).

[9] S. Srivastava, M. Vishnoi, M. T. Gangadhar, V. Kukshal, "An insight on powder mixed electric discharge machining: a state-of-the-art review", *Proc. Inst. Mech. Eng., Part B: J. Eng. Manuf.*, Vol. 237, No. 5, pp. 657-690, (2023).

[10] F. A. Olatz, A. S. Jose, and I. Borja, "Approaches for improvement of edm performance and for the understanding of electrode wear phenomena", *Precis. Eng.*,

Vol. 49, pp. 33-40 (2018).
[11] H. El-Hofy, H. Youssef, "Environmental hazards of nontradi*tio*nal machining", *Proc. of the 4th IASME/ WSEAS Int. Conf. on Energ. & Env. (EE'09)*, Cambridge, Vol. 24, No. 26, pp. 140–145, (2009).
[12] A. Rugbani, "Predictive model for diameter control of polysulfone hollow fibers produced by dry-jet wet spinning", *J. comput. appl. res. mech. eng. (JCARME)*, Vol. 13, No.1, pp. 27-38, (2023). https://jcarme.sru.ac.ir/article_1903.html.
[13] G. S. Chetan, P. V. Rao, "Environment-friendly machining of ni–cr–co based super alloy using different sustainable techniques", *Mater. Manuf. Processes,* Vol. 31, No. 7, pp. 852–859, (2016).
[14] D. Mabbu, R. P. Srinivasa, V. P. Madar, "Experimental investigation of edm process parameters by using pongamia pinnata osil blends as dielectric medium", *J. of Comput. & Appl. Res. in Mech. Eng. (JCARME)*, Vol. 11, No. 1, pp. 47-56, (2021).
[15] N. K. Singh, P. M. Pandey, K. K. Singh, M. K. Sharma, "Steps towards green manufacturing through edm process: a review", *Cogent Eng*, Vol. 3, No. 1, pp. 1–13, (2016).
[16] A. Al-Khazraji, S. Amin and S. M. Ali, "Study the effect of the graphite powder mixing electrical discharge machining on creation of surface residual stresses for aisi d2 die steel using design of experiments", *Eng. and Tech. J.*, Vol.33, Part (A), No.6, pp. 1399-1415, (2015).
[17] A. Kumar, S. Maheshwari, C. Sharma, N. Beri, "Research developments in additives mixed electrical discharge machining (AEDM): a state of art review", *Mater. Manuf. Process*, Vol. 25, No. 10, pp. 1166–1180, (2010).
[18] I. Shivakoti, G. Kibria, S. Diyaley, B. B. Pradhan, "Multi-objective optimization and analysis of electrical discharge machining process during micro-hole machining of D3 die steel employing salt mixed deionized water dielectric" *J. of Comput. & Appl. Res. in Mech. Eng. (JCARME)*, Vol. 3, pp. 27-39, (2013).
[19] M. Jose, S. P. Sivapirakasam, M. Surianarayanan, "Analysis of aerosol emission and hazard evaluation of electrical discharge machining (EDM) process", *Industrial Health*, Vol. 48, pp. 478-486, (2010).
[20] K. Dhakar, A. Dvivedi, "Dry and near-dry electric discharge machining processes", *Advanced Manufacturing Technologies. Materials Forming, Mach. and Trib.*, K. Eds. Gupta, Springer, Cham., pp. 249-266, (2017).
[21] V. S. Nimbalkar, P. M. T. Shete, "Experimental investigation of machining parameters using solid and hollow electrode for EDM of Ti-6Al-4V", *Int. Res. J. Eng. Technol*., Vol. 4, 2345, (2017).
[22] M. Shukla, K. Sharma, "Assessment of particle size distribution and tensile properties of hybrid epoxy composite reinforced with functionalized graphene and CNT nanofillers", *J. of Comput. & Appl. Res. in Mech. Eng. (JCARME)*, Vol. 12, No. 1, pp. 1-12, (2022).
[23] M. D. N. Islama, A. Dasa, S. Jarina, "Experimental Investigation of Mechanical Behavior of CFRP-AA7075-T6 Composite and Finite Element Analysis for Automotive Wheel Rim Application", *Journal of Materials and Engineering*, Vol. 02, Iss. 4, PP. 259-266, (2024).
[24]A. M. S. Kumar, "Microstructural Evaluation of Al-Al2O3 Composites Processed by Stir Casting Technique", *Journal of Materials and Engineering*, Vol. 02, Iss. 4, 267-272, (2024).
[25] X. Wang, S. Yi, H. Guo, C. Li, S. Ding, "Erosion characteristics of electrical discharge machining using graphene powder in deionized water as dielectric," *Int. J. Adv. Manuf. Technol*, Vol. 108, pp. 357-368, (2020).
[26] M. P. Jahan, P. Kakavand, F. A. Alavi, "A comparative study on micro-electro-discharge-machinedsurface characteristics of Ni-Ti and Ti-6Al-4V with respect to biocompatibility", *Procedia Manuf*., Vol. 10, pp. 232–242, (2017).
[27] M. A. Pathan, A. Kumar, and V. J. Badheka, "Recent advances in electrical discharge machine techniques and machining: a

review", *World J. of Adv. Eng. Tech. and Sci,* Vol. 12, No. 02, PP. 124–132, (2024)..
[28] M. Rahman, Z. G. Wang, Y. S. Wong, "A review on high-speed machining of titanium alloys", *In Proc. of the 3rd Int. Conf. on Leading Edge Man. in 21st Century*, Nagoya, Japan, Vol. 49, pp. 19–28, (2005).
[29] A. Hassan," Investigation on surface hardness and microstructure evolution in AA 7075-T651 multi-layered laminate fabricated through friction stir additive manufacturing", *IJMSE*, Vol. 20, No. 4, pp. 1-12, (2023).
[30] H. Hocheng, H. V. Tsai, "Advanced analysis of nontraditional machining", *Springer Science & Business Media*, Berlin/Heidelberg, Germany, (2013).
[31] A. Alidoosti, A. Ghafari-Nazari, F. Moztarzadeh, N. Jalali, S. Moztarzadeh, M. Mozafari, "Electrical discharge machining characteristics of nickel-titanium shape memory alloy based on full factorial design", *J. Intell. Mater. Syst. Struct.,* Vol. 24, pp. 1546–1556, (2013).
[32] S. L. Chen, S. F. Hsieh, H. C. Lin, M. H. Lin, J. S. Huang," Electrical discharge machining of TiNiCr and TiNiZr ternary shape memory alloys", *Mater. Sci. Eng. A*, Vol. 445–446, pp. 486–492, (2007).
[33] R. P. Sandeep, V. R. Vaira, V. Ajay, H. S. Harie, T. S. Vyoma, R. Padmanaban, R. Samuel, P. S. Kumar, "Influence of friction stir processing parameters on the mechanical and corrosion properties of Al-Cu-Li alloy", *IJMSE*, Vol. 20, No. 2, pp. 1-11, (2023).
[34] F. Mustafa, S. Daham, "Investigation of process parameters for T-joint aluminum alloy 6061-T6 with nanocomposites material friction stir welding based on the Taguchi method', *J. of Comput. & Appl. Res. in Mech. Eng. (JCARME),* Vol. 11, No. 1, pp. 101-111, (2021).
[35] M. Mustu, B. Demir, F. Aydin, H. Gürün, "An investigation of the PMEDM processing and surface characterizations of az61 matrix composites via experimental and optimization methods", *Mater. Chem. Phys.,* Vol. 300, 127526, (2023).
[36] Dunya. A. Ghulam and A. F. Ibrahim, "Enhancing electrical discharge machining performance by mixing nano chromium trioxide powder with soybean dielectric to machine inconel 718 alloy", *Adv. Sci. Technol. Res. J.,* Vol. 18, No. 2, pp. 129-142, (2024).
[37] S. Amirkhanlou, B. Niroumand, "Synthesis and characterization of 356-SiCp composites by stir casting and compocasting methods", *Trans. Nonferrous. Met. Soc*. Vol. 20, pp. 788-793, (2010).
[38] K. Dhakar, A. Dvivedi, "Parametric evaluation on near-dry electric discharge machining", *Mater. Manuf. Process*, Vol. 31, Vol. 4, 413–421, (2016).
[39] N. K. Singh, P. M. Pandey, K. K. Singh, "Experimental investigations into the performance of EDM using argon gas-assisted perforated electrodes", *Mater. Manuf. Process,* Vol. 32, No. 9, PP. 940–951, (2017).
[40] P. K. Gupta, A. Dvivedi, P. Kumar, "Effect of pulse duration on quality characteristics of blind hole drilled in glass by ECDM", *Mater. Manuf. Process*, Vol. 31, No. 13, pp. 1740–1748, (2016).
[41] X. Bai, Q. H. Zhang, T. Y. Yang, J. H. Zhang, "Research on material removal rate of powder mixed near dry electrical discharge machining". *Int. J. Adv. Manuf. Technol*. Vol. 68, pp. 1757–1766 (2013).
[42] L. Upadhyay, M. L. Aggrawal, P. M. Pandey, "Performance analysis of magnetorheological fluid-assisted electrical discharge machining. mater", *Manuf. Process.* Vol. 33, No. 11, pp. 1205–1213, (2018).
[43] M. D. Xames, F. K. Torsha, and F. Sarwar, "ANN-based performance prediction of electrical discharge machining of ti-13nb-13zr alloys", *World J. Eng*, Vol. 21 No. 2, pp. 217-227, (2024).
[44] C. Prakash, H. K. Kansal, B. S. Pabla, S. Puri, "Experimental investigations in powder mixed electric discharge machining of ti–35nb–7ta–5zrβ-titanium alloy", *Mater. Manuf. Process*, Vol. 32, No. 3, PP. 274–285, (2017).
[45] J. P. Agrawal, N. Somani, and N. K. Gupta, "A systematic review on powder-mixed electrical discharge machining

(pmedm) technique for machining of difficult-to-machine materials", *Innovation Emerging Technol.*, Vol. 11, 2440002, PP. 1-11, (2024).

[46] Y. F. Tzeng, and C. Y. Lee, "Effects of powder characteristics on electro-discharge machining efficiency" *Int. J. Adv. Manuf. Technol.* Vol. 17, pp. 586–592 (2001). https://link.springer.com/article/10.1007/s001700170142

[47] P. Kumar, M. Gupta, V. Kunar, "Experimental investigation of surface crack density and recast layer thickness of WEDMed Inconel 825", *J. of Comput. & Appl. Res. in Mech. Eng. (JCARME)*, Vol. 11 No.1, pp. 205-216, (2021). https://jcarme.sru.ac.ir/article_1372.html

[48] N. Pragadish and M. Pradeep Kumar, "Surface Characteristics Analysis of Dry EDMed AISI D2 Steel Using Modified Tool Design", *JMST*, Vol. 29, No. 4, pp. 1737-1743, (2014).

[49] A. Abdudeen, J. E. Abu Qudeiri, A. Kareem, T. Ahammed, A. Ziout, "Recent advances and perceptive insights into powder-mixed dielectric fluid of EDM", *Micromachines*, Vol. 11, pp. 754.

[50] S. Kumar, A. Batish, R. Singh and T. P. Singh, "A hybrid Taguchi-artificial neural network approach to predict surface roughness during electric discharge machining of titanium alloys," *JMST*, Vol. 28, No. 7, pp. 2831-2844, (2014).

[51] K. Paswan, A. S. Dube, S. Shankar, "Exploring powder mixed electrical discharge machining (PMEDM)" *AIP Conf. Proc.* Vol. 3178, No. 1, 070011, (2024)

[52] L. Q. Li, W. S. Zhao, S. C. Di, et al., "Experimental study on electrical discharge machining in gas", *JME*, Vol. 42, No. 203, (2006).

[53] L. Liqing and S. Yingjie, "Study of dry EDM with oxygen-mixed and cryogenic cooling approaches ", *Procedia CIRP*, Vol. 6, pp. 344–350, (2013).

[54] S. Jeavudeen, H. S. Jailani, and M. Murugan, "Powder additives influence on dielectric strength of EDM fluid and material removal" *Int. J. Mach. Mach. Mater.*, Vol. 22, No.1, pp. 47–61, (2020).